ELSEVIER

Journal of Chromatography B, 774 (2002) 53–58

JOURNAL OF CHROMATOGRAPHY B

www.elsevier.com/locate/chromb

Three-dimensional protein map according to p*I*, hydrophobicity and molecular mass

Daniel B. Wall, Stephen J. Parus, David M. Lubman*

Department of Chemistry, University of Michigan, 930 North University Avenue, Ann Arbor, MI 48109-1055, USA

Received 30 October 2001; received in revised form 12 March 2002; accepted 3 April 2002

Abstract

A three-dimensional method has been developed to map the protein content of cells according to p*I*, M_w and hydrophobicity. The separation of complex protein mixtures from cells is performed using isoelectric focusing (IEF) in the liquid phase in the first dimension, non-porous silica (NPS) RP-HPLC in the second dimension and on-line electrospray ionization (ESI) time-of-flight mass spectrometry (TOF-MS) detection in the third dimension. The experimentally determined p*I*, M_w and hydrophobicity can then be used to produce a three-dimensional map of the protein expression of a cell, where now each protein can be tagged by three independent parameters. The ESI-TOF-MS provides an accurate M_w for the intact protein while the hydrophobicity dimension results from the RP-HPLC component of the separation. The elution time, or percent acetonitrile at time of elution, of the protein is related to the hyrophobicity, which is an inherent property of the protein. 3D protein maps can thus be generated showing p*I*, M_w and % acetonitrile at time of elution as well as p*I*, M_w and hydrophobicity. The potential of the 3D plot for effective mapping of proteins from cells compared to current 2D methods is discussed.

Keywords: p*I*; Hydrophobicity; Molecular mass; Three-dimensional protein map; Proteins

1. Introduction

Currently most proteomic researchers use the p*I* and M_w of a protein to separate and image the protein content of a cell. This is widely performed using 2D gel electrophoresis as a means to separate proteins in a cell using p*I* in one dimension and SDS–PAGE gel electrophoresis in the second dimension. The 2D map that results can be used to map proteins in the cell according to p*I* and apparent M_w. The gel image is digitized and used to compare protein expression between cellular samples to search for changes that occur in cells. This method is valuable for detecting changes in cells that occur during cell transformation [1–3] or due to drug treatment for example [4,5]. In related work, there have been several attempts to develop protein maps using alternative methods, but still using the traditional p*I* versus M_w format [6–15].

In recent work, we have reported a 2D liquid separation method for separating large numbers of proteins from cellular lysates. This has involved liquid phase isoelectric focusing (IEF) separation in the first dimension, an RP-HPLC separation in the second dimension and on-line electrospray mass spectrometry in the third dimension. With the re-

*Corresponding author. Tel.: +1-734-764-1669; fax: +1-734-615-8108.

E-mail address: dmlubman@umich.edu (D.M. Lubman).

1570-0232/02/$ – see front matter
PII: S1570-0232(02)00189-7

sulting information a plot can be obtained of the cellular protein content in a three-dimensional format according to p*I*, M_w and hydrophobicity. The 3D method allows enhanced separations of large numbers of proteins and also a third dimension for tagging proteins for identification in interlysate comparisons. The method also provides enhanced capabilities for reproducibility based upon an accurate M_w of the intact protein as provided by ESI-TOF-MS and a highly reproducible hydrophobic separation. The 3D image is demonstrated for several hundred proteins from a human erythroleukemia (HEL) cell separation and various perspectives of the image are presented.

2. Experimental

2.1. HEL protein sample preparation

HEL cell-line samples were prepared in the lab of Dr Michael Long at the University of Michigan in the Department of Pediatrics as in previous work [14,15]. The proteins were extracted from the cells by thawing to room temperature and adding 3 vol. of lysis buffer consisting of 6 *M* urea (Bio-Rad), 2 *M* thiourea (Bio-Rad), 1% *n*-octyl β-D-galactopyranoside (Sigma), 6% ampholytes (Bio-Rad, 3/10), 10 m*M* (Tris[2-carboxyethyl]phosphine) (TCEP) (Pierce), 10 m*M* dithiothreitol (DTT) (Bio-Rad) and 10 m*M* phenylmethylsulfonyl fluoride (PMSF) (Bio-Rad) [14]. The samples contained ~5×10^6 cells per mg of sample. Previous analysis of these HEL cell lines by 2D SDS–PAGE [14,16] shows that these samples do not contain highly over-expressed proteins such as albumin which are often found in body fluids and may interfere with the analyses performed in this work.

2.2. IEF–NPS RP-HPLC–ESI-TOF-MS

The method used to generate the separations and mass spectra in this work are the same as those used in previous work [15]. Briefly the soluble protein lysate is loaded into the miniRotofor with 8 *M* urea (Bio-Rad), 1% *n*-octyl β-D-glucopyranoside, 2 m*M* TCEP (Pierce) and 6% carrier ampholytes (4/10, Bio-Rad). The miniRotofor is run at 10 °C for 5 h after which the p*I* focused protein pH fractions are harvested. The 20 fractions contained in the Rotofor were collected simultaneously, into separate vials, using a vacuum source attached by plastic tubing to an array of 20 needles, which were punched through a septum. The pH of the fractions was measured using a mini-pH electrode (PH/C 900, Amersham Pharmacia Biotech). The concentration of protein in each fraction was determined using the Bradford-based assay (Bio-Rad). Protein p*I* fractions were stored at −80 °C until loading to the non-porous RP-HPLC column.

The Rotofor p*I* fractions are then injected sequentially into the NPS RP-HPLC system and separated using binary water–acetonitrile gradients. The separations were performed as in previous work [15]. The 3×33-mm columns packed with 1.5-μm diameter non-porous silica ODS I particles (Eprogen) were used for protein separations. The use of 3-mm columns allowed for slower flow rates (0.2 ml/min) than the 4.6-mm columns used in earlier work [14], which is more compatible with the on-line ESI-TOF-MS detection. The eluent from the column is directed to a splitter where a suitable flow rate (0.1 ml/min) is diverted to the ESI-TOF-MS (LCT, Micromass, Manchester, UK). The slower flow rate allowed improved sensitivity in the ESI-TOF-MS detection. The protein multiply-charged umbrellas are then deconvoluted using Max-Ent (Micromass) software to generate the intact protein M_w data. These M_w data are then summed and entered to the LcpI program [14,15] for display in banding format and 2D imaging. The p*I*, M_w and percent acetonitrile data were then extracted from this 2D plot and replotted in the virtual 3D plots using Origin (Microcal) [15].

3. Results and discussion

In Fig. 1 is shown a 3D map of the proteins detected from the cytosolic fraction of an HEL cell lysate. This image has been formed according to the three experimental parameters used to separate the proteins, which include the p*I*, M_w and percent acetonitrile at time of elution. There are over 450 unique features in this image where each sphere corresponds to a unique protein. The relative inten-

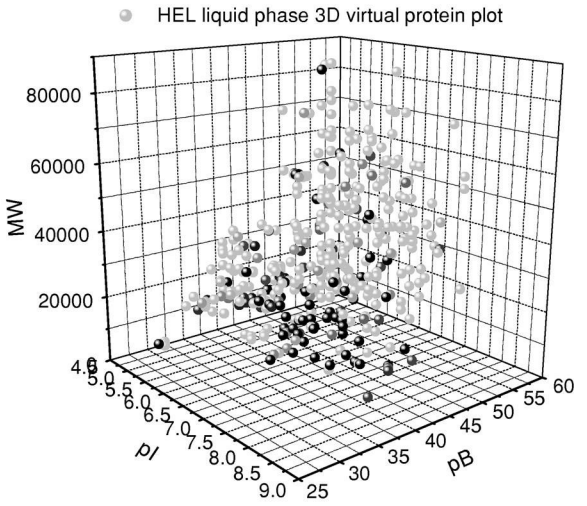

Fig. 1. 3D Protein plot according to p*I*, M_w and percent acetonitrile at time of elution.

sities of the peaks as determined using the detection of proteins by ESI-TOF-MS are represented by the gray scale color of the spheres. The proteins included in this image are mainly the more abundant proteins isolated from the cytosolic fraction, which have been detected over a p*I* range of 4–9 and a M_w range of 5–80 kDa. Additional proteins were detected at lower abundance or over an extended p*I* or M_w range, but were not included in this map.

The actual size of the spheres used in the 3D image are only for illustrative purposes and do not correspond to the true resolution available in the M_w dimension, where a resolution of close to 5000 (FWHM) is achieved. The exact M_w can be read from this image by clicking on the sphere and reading the *X*, *Y* and *Z* coordinates of that data point. Nevertheless, the use of a three-dimensional separation and image illustrates the potentially large field over which large numbers of proteins can be separated and displayed. In particular, the high resolution in the M_w dimension and the addition of the hydrophobic dimension allows the resolution of unique proteins which may not be separable on 2D gels. Of even greater importance is the reproducibility especially in the M_w dimension where absolute M_w becomes the parameter rather than electrophoretic mobility as in a gel. In comparison, 2D gels may not run the same depending on the gel conditions used, but the M_w value of a protein should always be the same within the mass accuracy of the instrument. The 3D plots are based upon M_w measurements that are accurate to 150 ppm, p*I* measurements accurate to 0.5 U and hydrophobicity measurements accurate to 0.035 U. The p*I* could be separated into narrower fractions (0.05 U) using commercial Rotolytes (Bio-Rad) in the buffer, where the entire pH range over the 20 fractions could be expanded over one pH unit. However, the 0.5 pH fractionation was found to be sufficient for this work.

In Fig. 2 is shown a 3D map of the HEL cell lysate mapped according to p*I*, M_w and hydrophobicity. The elution time of the protein in RP-HPLC is related to the hydrophobicity by the relationship noted in an earlier paper [15]. The percent acetonitrile at time of elution is related to the ratio of non-polar to polar amino acids. The hydrophobicity is an inherent property of the protein, which can be read directly from this image and would be more meaningful in terms of tagging these proteins. In addition, it would be a more reproducible parameter where the % B will vary according to the columns used and the gradient run. An important feature of this image is that it can be viewed from different directions, which might be used to study relationships in protein expression. This is shown for three different views of Fig. 2 in Figs. 3–5. In these images, it is possible to view various features of the

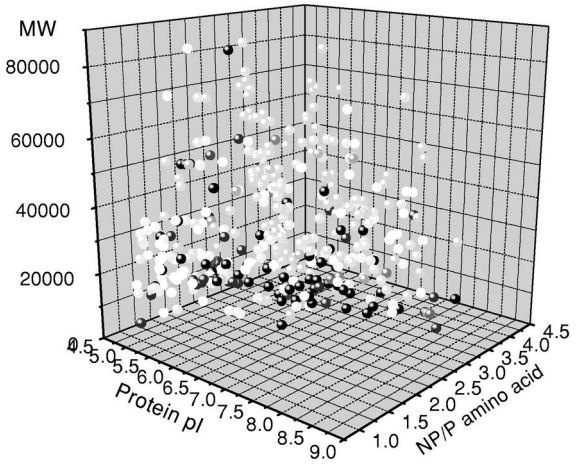

Fig. 2. 3D Protein plot according to p*I*, M_w and the hydrophobicity (NP/P amino acids).

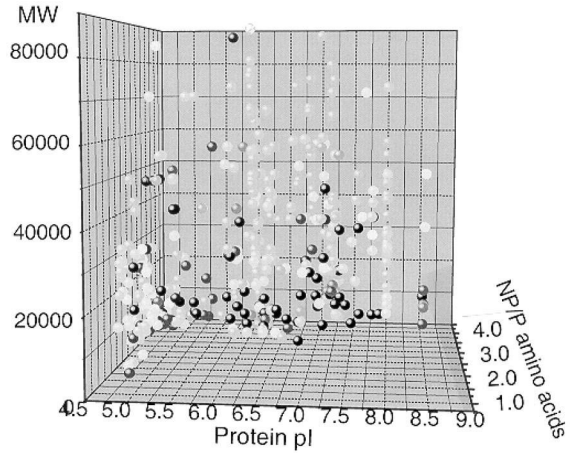

Fig. 3. pI–M_w view of Fig. 2.

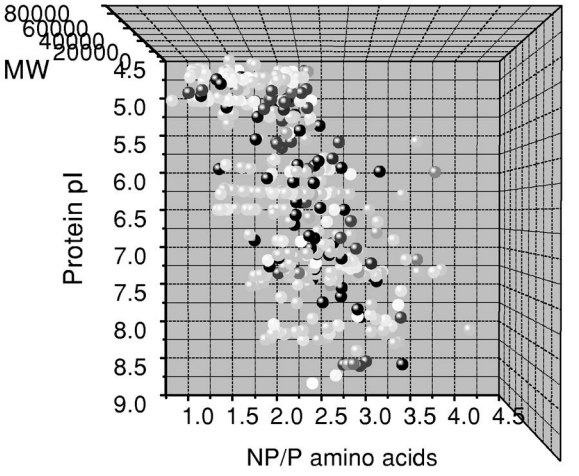

Fig. 5. pI–hydrophobicity view of Fig. 2.

image in detail by observing each of three 2D plots, these being M_w versus pI (Fig. 3), M_w versus NP/P (Fig. 4) and pI versus NP/P (Fig. 5).

The image of pI versus M_w (Fig. 3) is very similar to that of the traditional 2D gel separation. The main difference is that the mass resolution and mass accuracy of the data behind the plots are improved by 2 orders of magnitude compared to that of a gel.

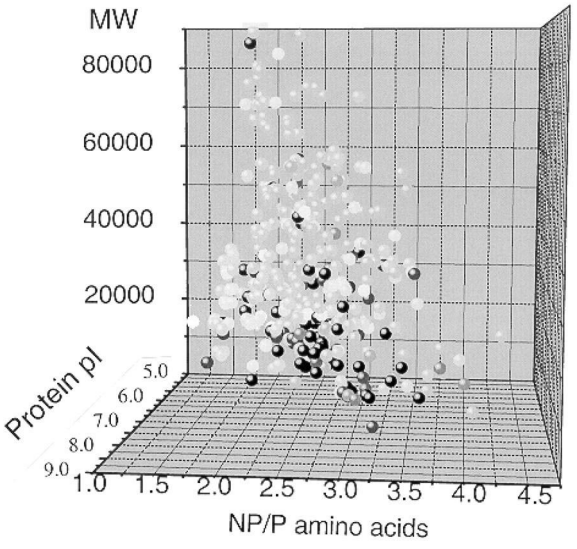

Fig. 4. M_w–hydrophobicity view of Fig. 2.

In a 2D gel the M_w measurement may only be accurate to ±5%. The accuracy for large proteins as measured in the ESI-TOF-MS has been shown to be better than 150 ppm [15]. It should be noted that in these images the relative shades of gray of the balls are related to the strength of the ESI signal detected. However, the ESI efficiency will vary for different proteins so that the figure in itself has no true quantitative significance. The quantitation will become significant in interlysate comparisons when the intensity of the same protein is compared in the different samples.

In comparison in Fig. 4 is shown a view of the image in terms of M_w versus hydrophobicity. The protein map shows that the larger the protein the lower the hydrophobicity. This is probably because larger hydrophobic proteins do not elute from the 1.5-μm NPS RP columns in the present gradient and are undetected by the mass spectrometer over the limited gradient used in these separations. Larger hydrophobic proteins have more recently been detected using this method with 3.0-μm NPS RP columns and a gradient up to 100% B [17]. Interestingly, the smaller proteins (<50 kDa) show a wider range of hydrophobicity indicating that not only is the ratio of NP/P amino acids important in the elution time of the protein, but also the total number of NP and P amino acids.

In Fig. 5 for example is shown the relationship

between p*I* and hydrophobicity. According to the protein map generated by this image, it appears that the more basic the protein the more hydrophobic it can be and still be detected by the mass spectrometer. The acidic mobile phase of the HPLC provides for enhanced solubilization of basic proteins where the acidic environment will protonate basic proteins more than acidic proteins. The increase in charge state for the basic proteins resulting from protonation makes them more soluble in the mobile phase of the RP-HPLC. The increase in charge state also makes these proteins less soluble in the stationary phase of the C_{18} packing material thus allowing them to elute earlier during the water–acetonitrile gradient.

4. Conclusions

The 3D protein map demonstrated herein offers an alternative method for mapping proteins according to p*I*, M_w and hydrophobicity. It offers a third dimension of separation for large numbers of proteins and the possibility for separating proteins that might coelute on a 2D gel, but would be separated in a 3D map based upon hydrophobicity or the high resolution of the M_w dimension. In addition, it may offer the advantage of reproducibility in interlysate comparisons in the M_w dimension as opposed to 2D gels where proteins may run differently in the electrophoretic mobility dimension depending on the conditions used. Indeed, one could conceive a map in shades of red for one cell lysate and another map in shades of green for a second cell lysate. The two 3D maps could be overlapped and compared for protein spheres that shift based upon the differential color scheme. The reproducibility and the accuracy of the p*I* dimension could be further improved by the use of other liquid p*I* based methods such as chromatofocusing [7] or immobilized isoelectric focusing membranes [10,18] which can provide improved fractionation over a narrower p*I* range ($<$0.2 p*I* units) with enhanced reproducibility. Also in these studies, the predictability of the elution time of a known protein can be useful in studies that involve the collection of target proteins for further analysis, where the target protein can be collected and other proteins ignored.

Acknowledgements

We gratefully thank Dr Tim Barder of Eprogen, Inc. for helpful suggestions during the course of this work. We would also like to thank Tim Riley and Matt Dilts of Micromass for loan of the LCT and Dr Michael Long in the Department of Pediatrics, School of Medicine, The University of Michigan, Ann Arbor, USA for sample preparation for this work. The authors gratefully acknowledge partial support of this work by the National Institutes of Health under grants No. R01 GM49500 and the National Science Foundation grant No. DBI-9987220.

References

[1] J.E. Celis, M. Ostergaard, H.H. Rasmussen, P. Gromov, I. Gromova, H. Varmark, H. Palsdottie, N. Magnusson, I. Andersen, B. Basse, J.B. Lauridsen, G. Ratz, H. Wolf, T.F. Orntoft, P. Celis, A. Celis, Electrophoresis 20 (1999) 300.
[2] M.J. Page, B. Amess, R.R. Townsend, R. Parekh, A. Herath, L. Brusten, M.J. Zvelebil, R.C. Stein, M.D. Waterfield, S.C. Davies, M.J. O'Hare, Proc. Natl. Acad. Sci. USA 96 (1999) 12589.
[3] A.C. Shaw, L.M. Rossel, P. Roepstorff, A. Holm, G. Christiansen, S. Birkelund, Electrophoresis 20 (1999) 977.
[4] C.S. Giometti, X. Liang, S.L. Tollaksen, D.B. Wall, D.M. Lubman, M. Vadrevu Subbarao, S. Rao, Electrophoresis 21 (11) (2000) 2162.
[5] L. Aicher, D. Wahl, A. Arce, O. Grenet, S. Steiner, Electrophoresis 19 (1998) 1998.
[6] C.L. Nilsson, T. Larsson, E. Gustafsson, K. Karlsson, P. Davidsson, Anal. Chem. 72 (2000) 2148.
[7] B.E. Chong, F. Yan, D.M. Lubman, F.R. Miller, Rapid Commun. Mass Spectrom. 5 (2001) 291.
[8] S. Udiaver, A. Apffel, J. Chakel, S. Swedberg, W.S. Hancock, W.S. Pungor, Anal. Chem. 70 (1998) 3572.
[9] P. Hoffmann, H. Ji, R.L. Moritz, L.M. Connolly, D.F. Frecklington, M.J. Layton, J.S. Eddes, R.J. Simpson, Proteomics 1 (2001) 807.
[10] X. Zuo, D.W. Speicher, Anal. Biochem. 284 (2) (2000) 266.
[11] R.O. Loo, T.I. Stevenson, C. Mitchell, J.A. Loo, P.C. Andrews, Anal. Chem. 68 (11) (1996) 1910.
[12] L. Yang, C.S. Lee, S.A. Hofstadler, L. Pasa-Tolic, R.D. Smith, Anal. Chem. 70 (1998) 3235–3241.
[13] P.K. Jensen, L. Pasa-Tolic, K.K. Peden, S. Martinovic, M.S. Lipton, G.A. Anderson, N. Tolic, K.K. Wong, R.D. Smith, Electrophoresis 21 (7) (2000) 1372.
[14] D.B. Wall, M.T. Kachman, S. Gong, R. Hinderer, S. Parus, D.E. Misek, S.M. Hanash, D.M. Lubman, Anal. Chem. 72 (6) (2000) 1099.

[15] D.B. Wall, M.T. Kachman, S. Gong, S.J. Parus, M.W. Long, D.M. Lubman, Rapid Commun. Mass Spectrom. 15 (2001) 1649.
[16] M.W. Long, C.H. Heffner, J.L. Williams, C. Peters, E.V. Prochownik, J. Clin. Invest. 85 (1990) 1072.
[17] K. O'Neill, D.M. Lubman, The University of Michigan, unpublished results, 2002.
[18] P.G. Righetti, A. Bossi, E. Wenisch, G. Orsini, J. Chromatogr. B 699 (1–2) (1997) 105.